minerals

MDPI

Article

Co-Precipitation of Cd, Cr, Pb, Zn, and Carbonates Using *Vibrio harveyi* Strain Isolated from Mediterranean Sea Sediment

Mazhar Ali Jarwar [1], Pablo Del Buey [2], M. Esther Sanz-Montero [2], Stefano Dumontet [1,*], Elena Chianese [3] and Vincenzo Pasquale [1]

[1] Laboratory of Environmental Microbiology, Department of Science and Technology, Parthenope University of Naples, Centro Direzionale, Isola C4, 80143 Naples, Italy
[2] Department of Mineralogy and Petrology, University Complutense Madrid, 28040 Madrid, Spain
[3] Laboratory of Environmental Chemistry, Department of Science and Technology, Parthenope University of Naples, Centro Direzionale, Isola C4, 80143 Naples, Italy
* Correspondence: stefano.dumontet@uniparthenope.it

Abstract: Heavy metal contamination is listed among the most alarming threats to the environment and human health. The detrimental effects of heavy metals in the natural environment span from a reduction of biodiversity to toxic effects on marine life—through microplastic born heavy metals, to impairment of microbial activity in the soil, and to detrimental effects on animal reproduction. A host of different chemical and biological technologies have been proposed to alleviate environmental contamination by heavy metals. Relatively less attention has been paid to the microbial precipitation of heavy metals, as a side mechanism of the most general process of microbially induced calcite precipitation (MICP). This process is currently receiving a great deal of interest from both a theoretical and practical standpoint, because of its possible practical applications in concrete healing and soil consolidation, and its importance in the more general framework of microbial induced mineral precipitation. In this study, we analyse the ability of the marine bacteria *Vibrio harveyi* in co-precipitating $CaCO_3$ minerals, together with Cd, Cr, Pb, and Zn added in form of nitrates, from solutions containing $CaCl_2$. The precipitated carbonatic minerals were a function of the different heavy metals present in the solution. The process of co-precipitation appears to be rather effective and fast, as the concentrations of the 4 heavy metals were reduced in 2 days by 97.2%, on average, in the solutions. This bioremediation technology could be used as environmental friendly procedure to de-contaminate suitable environmental matrices. The high performance of this process makes it particularly interesting for an upscaling from lab to field.

Keywords: heavy metals; microbially induced carbonate precipitation (MICP); bioremediation; calcite; vaterite

Citation: Jarwar, M.A.; Del Buey, P.; Sanz-Montero, M.E.; Dumontet, S.; Chianese, E.; Pasquale, V. Co-Precipitation of Cd, Cr, Pb, Zn, and Carbonates Using *Vibrio harveyi* Strain Isolated from Mediterranean Sea Sediment. *Minerals* **2023**, *13*, 627. https://doi.org/10.3390/min13050627

Academic Editor: Hiromi Konishi

Received: 23 March 2023
Revised: 22 April 2023
Accepted: 28 April 2023
Published: 29 April 2023

1. Introduction

The natural widespread occurrence of heavy metals in all the world's ecosystems is mainly due to the pedogenetic processes leading to the weathering of soil parent materials [1,2]. Thanks to such a process, living organisms are supplied with such elements, which are essential for their normal functioning [3]. Industrialized societies are responsible for increasing the environmental concentration of heavy metals, largely beyond their safe threshold levels, through wastes produced both by industrial and agricultural processes and household activities [4]. The high concentration of heavy metals found in the environment is responsible for severe toxic effects on exposed plants, animals, and humans. The detrimental effect of heavy metals is mainly due to their capability of combining with biomolecules, especially proteins, acting as potent enzyme inhibitors, hampering that way biochemical processes, and compromising the stability of genetic material and cell membrane integrity [5].

Heavy metals contamination is listed among the most alarming threat to the environment and human health [6]. Heavy metals have been classified as priority pollutants by most of the world's environmental protection agencies [7–11].

The detrimental effects of heavy metals in the natural environment span from a reduction of biodiversity [12]. Toxic effects on marine life through microplastic-borne heavy metals, to impairment of microbial activity in soil [13], to plant toxicity [14] and to various toxicological effects on fishes and animals, including the impairment of their reproductive potential [15,16]. An excellent review on the noxious effect of heavy metals on human health is reported by Jaishankar et al. [17].

Different chemical and biological technologies have been developed to alleviate environmental contamination by heavy metals. Among them, chemical precipitation, coagulation, flocculation, filtration, reverse osmosis, ion exchange, biosorption, aerobic and anaerobic microbial degradation were proposed by Abbas et al. [18] Focusing on biotechnologies, biosorption received particular attention for its effectiveness in the removal of metals from different environmental matrices and for its cost-effectiveness and eco-friendly nature [18,19].

However, relatively less attention has been paid to the microbial precipitation of heavy metal as a side mechanism of the most general process of microbial induced calcite precipitation (MICP). This process received a great deal of interest from both a theoretical and practical standpoint [20] and could assist in the endeavour of alleviating heavy metals contamination, by removing metals through their inclusion in carbonate minerals precipitated thanks to the microbial intervention. As far as soil contamination is concerned, ur Rehman et al. [21] suggested to stimulate soil cementation (the most important diagenetic process by which loose, scattered sand converts into tightly bound rock sandstone) through microbial activity, in order to obtain calcite minerals in which polluting heavy metals are incorporated. The MICP was applied even to de-contaminate mine tailings, a highly heavy metal polluted matrix. He et al. [22] succeeded in cementing tailings particles by MICP, sequestrating and passivating that way heavy metal ions into the calcite lattices. An additional threat to environmental integrity and food safety derives from the use of sewage sludge as fertilisers on agricultural fields [23]. The widespread sludge with heavy metal contamination can pollute groundwater through percolation [24], affect soil microflora impairing soil biological fertility and translocate heavy metal to plant tissues [23,25]. Zeng et al. [26] successfully used MICP treatment for the in-situ stabilization of heavy metals carried by an anaerobic digested sewage sludge, disposed to agricultural land. These authors were able to prevent the transfer of metals from the sludge to soil by reducing their soluble exchangeable fractions. Peng et al. [27] demonstrated the MICP effectiveness to both soil and water heavy metals decontamination.

The study of heavy metal co-precipitation has been interpreted as the result of various mechanisms, spanning from purely chemical reactions [28–32], to a process mediated by heterotrophic and photosynthetic microorganisms [33,34]. Wang et al. [35] reviewed, from a more practical point of view, the studies aimed at microbial induced carbonate precipitation for the immobilization of heavy metals, in an attempt to suggest an effective way to alleviate such an environmental threat. The critical point of all the studies reviewed by Wang et al. [35] remains the choice of a suitable microorganism able to induce a massive co-precipitation of carbonate and heavy metals.

The aim of this study was to analyse the feasibility of co-precipitate Cd, Cr, Pb, and Zn with carbonate minerals, thanks to the intervention of the bacteria Vibrio harveyi, from solutions containing $CaCl_2$ and Cd, Pb, Cr, and Zn in form of nitrates. The effectiveness of such an attempt was proved by the substantial reduction of heavy metals in the solutions and the production of different carbonates, as a function of the different metals. The strain of V. harveyi used here shoved the ability to precipitate massive amounts of carbonates in a short time.

2. Materials and Methods

2.1. Isolation of Heterotrophic $CaCO_3$ Biomineralizing Bacteria Strain

The bacterial strain of *Vibrio harveyi* used in this study was isolated from sea sediment collected on the coastline of the city of Pozzuoli (Gulf of Naples, Southern Italy), an area subjected to a severe heavy metal contamination in the recent past [36]. Three g of sediment were inoculated in a tube containing Precipitation Broth Medium (PBM) containing 3 $g \cdot L^{-1}$ of nutrient broth (Oxoid, Basingstoke, Hampshire, UK), 2 $g \cdot L^{-1}$ of NaCl (Oxoid, Basingstoke, Hampshire, UK), 36.68 g/L $g \cdot L^{-1}$ of $CaCl_2 \cdot 2H_2O$ (Sigma-Aldrich, Darmstadt, Germany), and 20 $g \cdot L^{-1}$ of urea (Bio-Rad Laboratories, Hercules, CA, USA). The broth culture was incubated aerobically at 30 °C in static conditions until the formation of crystals was visible to the naked eye. The supernatant and the sediment were then removed and the tube was washed 3 times with sterile saline solution (0.9% NaCl). Five more ml of saline solution were then added and the crystals adhering to the surfaces of the test tube were detached and fragmented with a sterile spatula. After vortexing for 1 min, a suspension loopful was streaked onto plates of TSA-Ca. The TSA-Ca was composed of Tryptone Soya Agar (Oxoid, Basingstoke, Hampshire, UK) supplemented with 1 $g \cdot L^{-1}$ of $CaCl_2 \cdot 2H_2O$. After incubation at 30 °C for 48 h, bacterial colonies showing the crystal formation were selected and purified on Trypton Soy Agar (Oxoid, Basingstoke, Hampshire, UK). After incubation, one of the grown colonies was biochemically characterized and molecularly identified.

2.2. Biochemical Characterization and Molecular Identification of Bacterial Strain

2.2.1. Urease Activity

Qualitative urease activity was performed by inoculating the strain into Urea Indole Medium (Bio-Rad Laboratories, Hercules, CA, USA) and incubating at 30 °C for up to 3 days in aerobic conditions. The microorganisms producing the urease enzyme, released ammonium from the hydrolysis of the urea inducing a color change from yellow to red-fuchsia in the medium.

2.2.2. Carbonic Anhydrase Assay

A carbonic anhydrase (CA) assay was performed by using cellulose disks (∅ 5 mm) containing 0.0067 g of p-nitrophenyl-acetate (p-NPA). Briefly, 0.1 g of p-NPA (Sigma-Aldrich, Darmstadt, Germany) was dissolved in 3 ml of absolute ethanol; blank antimicrobial susceptibility disks (Oxoid) were soaked with 20 µl of the p-NPA solution, left to dry at 37 °C.

The CA assay was performed by placing a disk near the colony of the selected bacterial strains grown in TSA at 30 °C for 48 h. The CA-producing bacteria, by inducing the cleavage of p-NPA to p-nitrophenol and acetate, produces the yellowing of the disk and the surrounding area within 5 min.

2.2.3. Molecular Identification of Bacterial Strain

The selected strains were identified using PCR amplification and direct Sanger sequencing of the 16S ribosomal RNA gene. DNA was extracted from colonies grown on TSA using Lyses & PCR-GO Kit (Bacteria/Fungi) following the manufacturer's instructions. PCR amplification was carried out by sequencing the 16S rRNA gene (region V1-V6) using universal primers 63f (5′-CAG GCC TAA CAC ATG CAA GTC-3′) for the forward primer and 1387r (5′-GGG CGG WGT GTA CAA GGC-3′) for the reverse primer [37]. PCRs were performed with the following conditions: initial denaturation at 98 °C for 5 s, followed by 35 cycles of denaturation at 98 °C for 5 s, annealing at 55 °C for 5 s, and extension at 72 °C for 18 s; final extension at 72 °C for 45 s.

Sanger sequencing was performed by using a 3130 Genetic Analyzer (Life Technologies o Applied Biosystems, Carlsbad, CA, USA). A sequence similarity search was performed using the BLAST algorithm against the GenBank database (http://blast.ncbi.nlm.nih.gov/Blast.cgi).

2.3. Heavy Metal Bio-Precipitation

In order to check the heavy metal resistance of the bacterial strain selected for this experiment, colonies of *V. harveyi* grown on TSA, after incubation at 30 °C for 24 h, were suspended in Nutrient Broth (Oxoid, Basingstoke, Hampshire, UK), spiked with 100 ppm of the single heavy metal used here. *V. harveyi* cells were added to the solutions up to reach a McFarland standard of 0.5 and then incubated for 48h at 30°C.

Colonies of *V. harveyi* grown on TSA, after incubation at 30 °C for 24 h, were suspended in the sterile saline solution until the McFarland turbidity standard no 2 was reached. Then, 20 µL of the cell suspension were inoculated in triplicate test tubes containing 10 mL of liquid medium, made by Nutrient Broth (Oxoid, Basingstoke, Hampshire, UK) 3 $g \cdot L^{-1}$, urea (Oxoid, Basingstoke, Hampshire, UK) 20 $g \cdot L^{-1}$, $CaCl_2 \cdot 2H_2O$ (Sigma-Aldrich, Darmstadt, Germany) 18.34 $g \cdot L^{-1}$, NaCl (Oxoid, Basingstoke, Hampshire, UK) 20 $g \cdot L^{-1}$. To these media, 100 ppm of Cd, Pb, Cr, and Zn, in form of NO_3^- (Sigma-Aldrich, Darmstadt, Germany), were singularly added. A treatment containing all the tested heavy metals, at a concentration of 100 ppm of each metal was also made. Treatments containing each one of the heavy metals tested, with no microbial inoculation, were used as a negative control. All the cultures were incubated, aerobically and in a static condition, for 10 days at 25 °C.

After incubation, the broth cultures were centrifuged and the supernatant was collected to determine the concentration of heavy metals. The crystals adhering to the surfaces and the crystals precipitated on the bottom of the test tubes were collected to carry out mineralogical characterization and SEM observations.

2.4. Metal Concentrations

Supernatants were filtered through 0.2 µm pore-size acetate filters and then digested with H_2O_2 under UV radiation. These solutions were analyzed for dissolved Cd^{2+}, Cr^{2+}, Pb^{2+}, and Zn^{2+} content by voltammetric analysis carried out with a Metrohm 797 VA Computrace equipped with a multimode working Mercury electrode (Anodic stripping voltammetry -ASV with the hanging mercury drop electrode - HMDE). An Ag/AgCl electrode and a Pt electrode were used as reference and auxiliary electrode respectively. For calibration, the standard addition method was applied to limit the matrix effects. All elements were quantified using linear regression; quality control and method's accuracy were as reported in Chianese et al. [38].

Pb concentration analyses of calcite crystals were carried out by interaction with hydrogen peroxide to remove organic matter prior to nitric acid digestion of the carbonate. Pb was analyzed using SPECTRO Arcos inductively coupled optical emission spectrometer (ICP-AES). This equipment has a simultaneous optical system Paschen-Runge with 32 detectors CCD and operates at 0.7–1.7 kW that covers a range of wavelengths comprised between 130 and 777 nm. The nebulizer flow is 0.95 mL/min. The analyses were carried out for Pb only due to the extremely fine dimension of crystals in the other experiments, which prevented the necessary quantity of material from being obtained.

2.5. X-ray Diffraction and SEM Analysis

Crystal adhering on the surfaces and the crystals precipitated on the bottom of the test tubes were examined through random powder X-ray diffraction (XRD) analysis using a Bruker D8 Advance diffractometer with Cu Kαradiation (λ = 1.54060 °A) and equipped with a Sol-X detector (Bruker, Biller-ica, MA, USA). The samples were scanned in a range 2θ from 2 to 65° with a step size of 0.02° 2θ per 0.5 s. In the case of non-purified extracellular polymeric substances (EPS), the counting time per step was 3 s. 3 Match (Crystal Impact) software was used for XRD interpretation.

Textural features and mineral assemblages were established by scanning electron microscopy using images recorded with secondary and backscattered electrons, and energy dispersive X-ray systems (EDX). Some freshly fractured surfaces of representative samples were air-dried and coated with Au under vacuum conditions at 25 mA. Scanning electron

microscopy observations were performed using JEOL JSM-7600F Field Emission scanning electron microscopy (FESEM), (JEOL USA Inc., Peabody, MA, USA).

3. Results and Discussion

V. harveyi was collected in the sea sediments of the coastline of the city of Pozzuoli (Gulf of Naples, Southern Italy), an area subjected to a severe heavy metal contamination in the recent past for being exposed for decades to the pollution generated from a steel factory [36]. Our choice to isolate a bacterium from such an environment aimed at isolating a bacterial strain able to withstand high heavy metal concentrations. Such a strain can be used in remediation of highly contaminated environmental matrices. *V. harveyi* showed a remarkable heavy metal resistance being able to grow and carry out MICP in presence of 100 ppm of the heavy metals here studied. After 48 h of incubation in presence of all the single heavy metals studied, the *V. harveyi* cultures reached a McFarland standard turbidity of 2.0, demonstrating the heavy metal tolerance of this bacterium to the maximum heavy metals concentration used here.

V. harveyi has been proven to be able to expressing both urease and carbon anhydrase activities. The expression of these two enzymes is often correlated to MICP enhancement by alkalinization of the medium [39–43].

Table 1 shows the amount of heavy metals left in the solutions along the incubation. The efficiency in heavy metal removal varied according to the different heavy metals studied (Cd > Cr > Pb > Zn). At day 2 of incubation only 2.28% (±3.5 sd) of all metals remained in solution. Zn was the poorly removed among metals and an increase of its concentration in solution was recorded at day 7 and 10, when it reached a value 2.4 times higher than that recorded at day 2. This phenomenon was also observed for Cr, as the concentration in the solution was 15.5 higher at day 10 compared to day 2. The concentration of Pb in the solution was 1.3 time higher at day 10 compared to day 2, whereas for Cd this value was 0.6.

Table 1. The concentrations of heavy metals in the supernatant of the broth cultures of *V. harveyi* along the incubation.

Incubation Time (day)	Zn^{2+} (mg/L)	% of Zn^{2+} Left in Solution	Cr^{+} (mg/L)	% of Cr^{2+} Left in Solution	Cd^{2+} (mg/L)	% of Cd^{2+} Left in Solution	Pb^{2+} (mg/L)	% of Pb^{2+} Left in Solution
D_0	107.78	100.0	72.13	100.0	131.32	100.00	72.00	100.00
Std	±1.948		±1.616		±0.629		±1.667	
D_2	8.19	7.60	0.44	0.60	0.41	0.30	0.43	0.90
std	±0.30		±0.08		±0.04		±0.026	
D_7	12.80	11.90	0.78	1.10	0.23	0.20	0.81	1.10
std	±0.26		±0.17		±0.01		±0.06	
D_{10}	20.02	18.60	0.53	9.30	0.17	0.17	0.84	1.20
std	±0.86		±0.11		±0.03		±0.04	

The apparent contradictory results, showing an increase of some heavy metal concentrations in the solution, have a possible explanation in the known ability of microorganisms to both precipitate and dissolve minerals. As matter of fact, evident marks of calcite crystal partial dissolution were evident in the SEM micrographs, as showed in Figures 1A, 2A and 3C. Our findings seem to be in agreement with those of Jacobson and Wu [44], who, worked with the heterotrophic bacterial species *Burkholderia fungorum*, found that the microbially induced calcite crystals produced were dissolved by both the H_2CO_3 generated by dissolution of atmospheric CO_2 in their reacting media (according to the equation $H_2CO_3 + CaCO_3 = Ca^{2+} + 2HCO_3^-$) and H^+ released during NH_4^+ bacterial uptake (according to the equation $H^+ + CaCO_3 = Ca^{2+} + HCO_3^-$). Considering the presence of urea in our reaction media, as well as the ureolytic activity showed by *V. harveyi*, the mechanism proposed by Jacobson and Wu [44] could have outpaced the precipitation of $CaCO_3$ in the short run. It is interesting to note that this phenomenon occurs in different kinetics as function of the different heavy metals used here. Similarly, Perito and Mastromei observed that formation of calcite crystals, in presence of gypsum and *Desulfovibrio* spp., occurs

by a combination of dissolution–precipitation and diffusion processes based on gypsum dissolution and subsequent calcite formation [45].

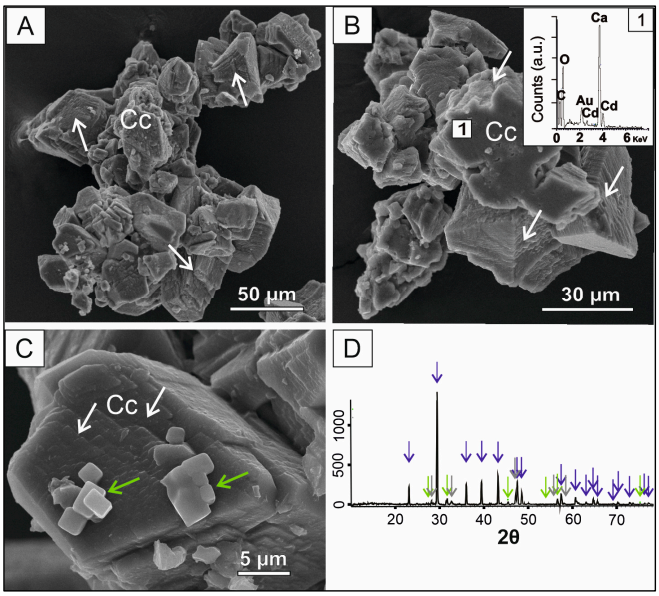

Figure 1. Scanning electron microscope micrographs showing aggregates of calcite crystals. (**A**) Arrows show signs of calcite crystal dissolution. (**B**) EDX spectrum of the surface of a calcite crystal formed from Cd-spiked solutions (1). (**C**) Calcium fluoride cubic crystals (green arrows) on the surface of a calcite crystal (white arrows). (**D**) X-ray diffraction pattern of precipitates fromed in Cd-spiked solutions: calcite (blue arrows), halite (green arrows), and calcium fluoride (grey arrows). Cc = calcite crystals.

In addition, the coupled dissolution-crystallization reactions were frequently observed in both surface and subsurface geological environments, involving different carbonate minerals, neo-formed bio-mineral included [32,46,47].

A possible mechanism driving microbially mediated calcite precipitation has been identified in the diffusion of positively charged Ca^{2+} ions from the solution to the cell surface and their bonding to negatively charged functional groups of extracellular polymeric substances (EPS) [9]. These same EPS appear to be able to promote mineral dissolution as well [48]. In other words, the microbes-mineral interplay seems to be characterized by an incessantly alternation of mineral precipitation-mineral dissolution-release of ions-mineral precipitation ad so on. The intriguing thing is that such a process can be mediated through the same compounds: EPS for calcite, and organic acids for clay minerals [49–51].

Two polymorphs of $CaCO_3$ (calcite and vaterite) were precipitated in different proportions in the experiments. Remarkably, the experiments produced calcite when Cd, Cr, and Pb were concerned, whereas in the Zn experiment vaterite was the dominant mineral phase, suggesting that heavy metals co-precipitate with carbonates which incorporate in the crystal structure (i.e., replacing Ca in the crystal lattices) of the new mineral phase. In case of Zn, this precipitation may influence the $CaCO_3$ polymorph selection leading to vaterite stabilization and partial calcite dissolution with consequent release of Zn into the solution.

In the control experiment both the $CaCO_3$ and heavy metals precipitation were not observed. Thus, the halophilic *V. harveyi* seems to have played a role in the production of calcite and vaterite in our reaction media. *V. harveyi* is a well-known hyperhalophilic bacteria whose ability to precipitate calcite was reported under extreme halophilic conditions [51,52]. According to our results, this bacterium seems to be able inducing MICP also in non-halophilic media. This characteristic could potentially enhance the use of *V. Harvey* in bioremediation technologies by widening the environmental conditions in which it could operate.

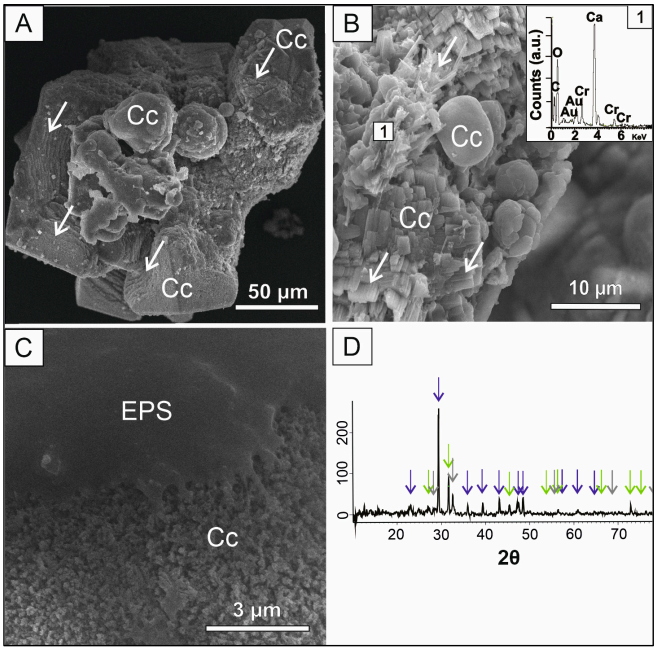

Figure 2. Scanning electron microscope micrographs showing aggregates of different morphologies of calcite crystals precipitated from Cr-spiked solutions. (**A**) Dissolution marks in rhombohedral crystals of calcite where globular crystals grow on deeply etched surfaces of the former. (**B**) Detail of dissolution edges on rhombohedral calcite crystals and their close relationship with globular carbonates. EDX spectrum of dissolved surfaces of calcite crystals formed from Cr-bearing solutions (1) (**C**) Close micrograph of rugose calcite surface associated to extracellular polymeric substances (EPS). (**D**) X-ray diffraction pattern of precipitates: calcite (blue arrows), halite (green arrows), and calcium fluoride (grey arrows). Cc = calcite crystals; EPS = bacterial esopolysaccharides.

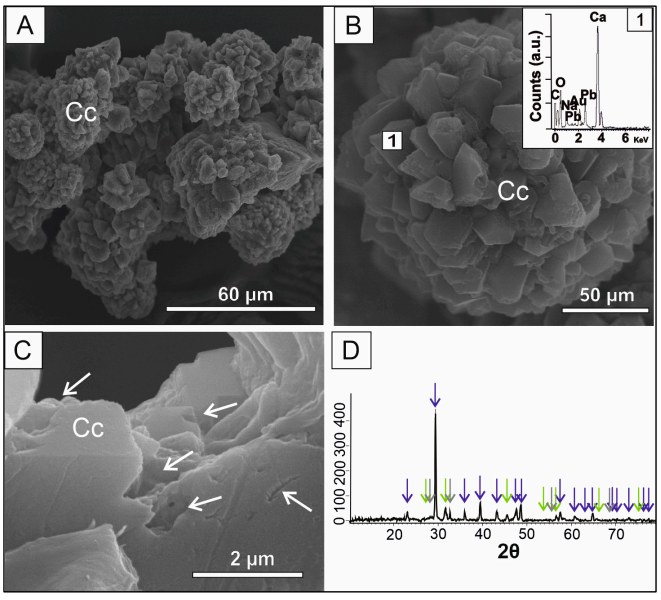

Figure 3. SEM micrographs showing aggregates of calcite crystals precipitated from Pb-spiked solutions. (**A**) Idiomorphic rhombohedral calcite crystals aggregates. (**B**) Spherical idiomorphic calcite crystal aggregate and EDX spectrum of alterated surfaces of calcite crystals. (**C**) Detail of dissolution marks on calcite crystal edges. (**D**) X-ray diffraction pattern of precipitates formed within Pb-spiked solutions: calcite (blue arrows), halite (green arrows), and calcium fluoride (grey arrows). Cc = calcite crystals.

Table 2 compares the efficiency of heavy metal removal by different bacterial strains, inducing MICP and co-precipitating heavy metals from solutions containing $CaCl_2$. The interest in using Vibrio harveyi strain in this context lies in its high resistance to detrimental effect of such pollutants. In our study we used a concentration of Zn, Cd, Cr, ad Pb equal to 100 ppm, among the highest reported in scientific litterature. As reported in Table 2, Sharma et al. [53] used an incredible high concentration for Pd and Cr (2000 ppm) being, to our best knowedge, the only case in which a such high amount of metals has been applied. Mwandira et al. [54] and Mugwar and Harbottle [55] used a concentration of 100 ppm only for Pb, whereas the in the other studies the concentration of heavy metals spanned for 1.2 to 22.3 ppm.

Table 2. Efficiency of heavy metal removal (laboratory experiments) by different bacterial strains inducing MICP and co-precipitating heavy metals from solutions containing $CaCl_2$.

Strain	Incubation Time	Removal Efficiency (%)	[1]Max Heavy Metal Concentration (ppm)	Reference
Vibrio harveyi	2 days	92.4 (Zn); 99.4 (Cr); 99.6 (Cd); 99.1 (Pb)	100.0 (Zn, Cd, Cr, Pb)	This study
Pararhodobacter sp	6 h	100 (Pb)	103.6 (Pb)	[54]
Sporosarcina pasteurii	7 days (Zn); 7 days (Pb); 3 days (Cd); 3 days (Cd);	100 (Zn); 100 (Cd); 100 (Zn); 99 (Pb); 65 (Cu)	10.4 (Zn); 31,1 (Cd); 103.6 (Pb); 3.2 (Cu)	[55]
Terrabacter tumescens	48 h	90–99% (Pb Cd, Ni, Cu, Co, Zn)	1.2 (Ni); 1.3 (Cu); 4.2 (Pb); 1.2 (Co); 1.3 (Zn); 2.3 (Cd)	[56]
Sporosarcina pasteurii	2 weeks	60 (Cu); 30 (Zn); 95.4 (Pb) 60 (Cd)	0.06 (Cu); 0.3 (Zn); 20.7 (Pb); 0.6 (Cd)	[57]
Sporosarcina pasteurii	240 h	98.7 (Pb); 97.1 (Cd); 94.8 (Zn)	22.5 (Pb; Cd; Zn)	[58]
Sporosarcina pasteurii	18 days	92.0 (Pb); 94 (Cr)	2000.0 (Pb and Cr)	[53]
Sporosarcina pasteurii	[4]NA	95.6 (Zn); 81.5 (Mn); 99.6 (Cu);	[3]4.4 (Cu); [3]3.8 (Zn); [3]2.8 (Pb); [3]10.8 (Mn)	[59]
Stenotrophomonas rhizophila *Variovorax boronicumulans*	240 h	[4]96.1 (Pb); [4]72.4 (Cd); [4]68.9 (Zn)	22.5 (Pb; Cd; Zn)	[58]
Staphylococcus epidermidis	5 days (Pb); 6 days (Cd)	86.0 (Pb); 76.8 (Cr)	1.1 (Pb); 3.2 (Cr)	[60]

[1] Maximum heavy metal concentration at which co-precipitation occurs. [3] Values estimated from plotted results. [4] Average values for both *Stenotrophomonas rhizophila* and *Variovorax boronicumulans*.

3.1. Cd Mediated Co-Precipitation

Identification and morphological characterization of $CaCO_3$ precipitates were based on XRD data (Figure 1D) and scanning electron microphotographs (Figure 1A–C). Calcite was the only $CaCO_3$ polymorph resulted from the Cd spiked solutions. The majority of calcite crystals exhibited typical rhombohedral morphology, whereas only some of them were prismatic. Crystal dissolution marks, such as irregularly dissolved crystal faces and edges that obliterate the external morphology, are frequently observed (Figure 1A). Pérez-Garrido et al. [30] established that a Cd critical concentration exists that affects calcite dissolution regime at higher impurity concentrations. Cd content estimated by SEM-EDX varies from 0.04 to 1.08% wt. The adsorption of Cd on calcite crystal faces is a Cd removal secondary process regarding the low Cd concentration on the surface. This assumption can be extended to the other heavy metals (i.e., Cr, Pb and Zn) tested in this study.

3.2. Cr Mediated Co-Precipitation

Chromium-bearing carbonate crystals exhibit a more diverse variety of crystal morphologies than those showed by crystal formed in the Cd-spiked solutions (Figure 2), as rhombohedral and globular shaped crystals were found. Deep alteration marks were largely visible on the edges and faces of rhombohedral crystals. Complex aggregates of globular crystals grow on the dissolved faces commonly forming complex aggregate suggesting that globular calcite grows at expenses of dissolved rhombohedral calcite. Sánchez-Pastor et al. [31] reported an inverse morphological growth pathway in presence of Cr (VI) where calcite spheres dissolved at expense of rhombohedral crystals. Another significant difference in relation to the present study is the stabilization of vaterite at a high concentration of Cr (VI) [29]. The Cr content measured by EDX varies greatly along crystal surfaces (0.21–3.25% wt). Halite and calcium fluoride were also detected by the XRD analysis (Figure 2D).

3.3. Pb Mediated Co-Precipitation

Lead-bearing carbonates consist basically of spherical aggregates of rhombohedral calcite crystals (Figure 3), often coalescing and forming more complex groups. SEM microphotographs reveal irregular dissolution features on rhombohedral crystal faces and edges. The Pb content of such crystals, analyzed by SEM-EDX, varies greatly (0.11–1.53% wt). Digestion analyses of calcite crystals revealed Pb concentration values of up to 41 ± 1 ppm. This concentration explains the slightly shifting of the reflections to higher d-spacing values in contrast to other heavy metal-bearing calcite diffractograms (Figure 3D). In contrast to other inorganic mechanisms of Pb interaction with calcite [32]. *V. harveyi* metabolism induces Pb-bearing calcite without the presence of secondary lead carbonates (i.e., cerussite and hydrocerussite). In parallel to Cd experiments reported before, dissolution features are observed on the edges of Pb-bearing calcites (Figure 3C). A threshold of Pb concentration in bio-induced calcites can be established based on these experiments (i.e., ±40 ppm). In contrast to Cr-bearing cultures, no crystal morphological changes were identified for Cd and Pb.

3.4. Zn Mediated Co-Precipitation

Zn differed from the other heavy metals experiments (i.e., Cd, Cr and Pb) in $CaCO_3$ polymorph dominant phase (Figure 4). Up to 80% of the sample consists of vaterite, being calcite residual. To best of our knowledge, this is the first work that biogenic vaterite is stabilize in a Zn doped medium in the presence of the gram-negative bacteria *Vibrio haveyi*. Precipitation of biogenic vaterite was stabilized before by microbial culture of gram-positive bacteria *Bacillus subtilis* in the presence of Cd, Ni and Cu [61]. Vaterite exhibits a typical globular crystal morphology, those micrometer crystalline aggregates other are embedded in the bacterial-formed biofilms (Figure 4C). The Zn content of vaterite surfaces varies in the same line as in the case of Pb (0.08–1.52% wt).

In our solutions containing *V. harveyi* and Cr, the co-precipitation with calcium carbonate produced calcite and not vaterite. These findings are not in agreement with those of Sánchez-Pastor et al. [31] and Cruz et al. [29], who reported, based on abiotic experiments, that Cr, co-precipitating with calcium carbonate, was incorporated into vaterite crystal lattice as anionic group (i.e., tetrahedral chromate) substituting triangular carbonate groups [62]. Whereas, in our microbial cultures, it seems that Cr was incorporated into calcite crystal structure by replacing Ca ions, as it was in Cd and Pb experiments. In other words, Cr, Cd, and Pb co-precipitate with calcite (i.e., chemical species that directly come from aqueous solution incorporated into carbonate structure). These divalent metals (Cr, Cd, and Pb) are rapidly removed from the solution in the initial stages of co-precipitation followed by a much lower uptake that comes along with crystal dissolution mechanisms. Pérez-Garrido et al. [30] observed that long-term uptake of divalent heavy metals (i.e., Cd) seems to occur through a dissolution-crystallization mechanism and, to a much lesser extent, through metal adsorption to calcite surface. The results of dissolution-crystallization precipitation process are reflected in the inner zonation of carbonate crystals, where the inner part is chromium-rich [31]. On the other hand, Zn has the same effect as the chromate anionic group by stabilizing vaterite over calcite [29]. No other heavy metal-bearing carbonate phases such as hydrocerussite or cerussite have been precipitated by *V. harveryi* in contrast to other abiotic Pb-bearing carbonate experiments [32].

The microanalyses, carried out on calcite containing Pb, demonstrated that calcite incorporated Pb during its crystal growth, leading to hypothesizing the same process for Cd and Cr, and for Zn in the case of vaterite. The precipitation of biogenic metastable vaterite favored by the substitution of Ca by Zn by Vibrio haveryi is, to the best of our knowledge, the first report of a biogenic vaterite in the presence of Zn. Previously, Liu & Lian [61] precipitate biogenic vaterite doped with Cd, Ni and Cu in the presence of Bacillus subtilis. Furthermore, these observations are in agreement with those of Navrotsky (2004) [63] and Radha et al. [64], who argued that certain impurities could play a role in the inversion of the energetic stability between the $CaCO_3$ polymorphs.

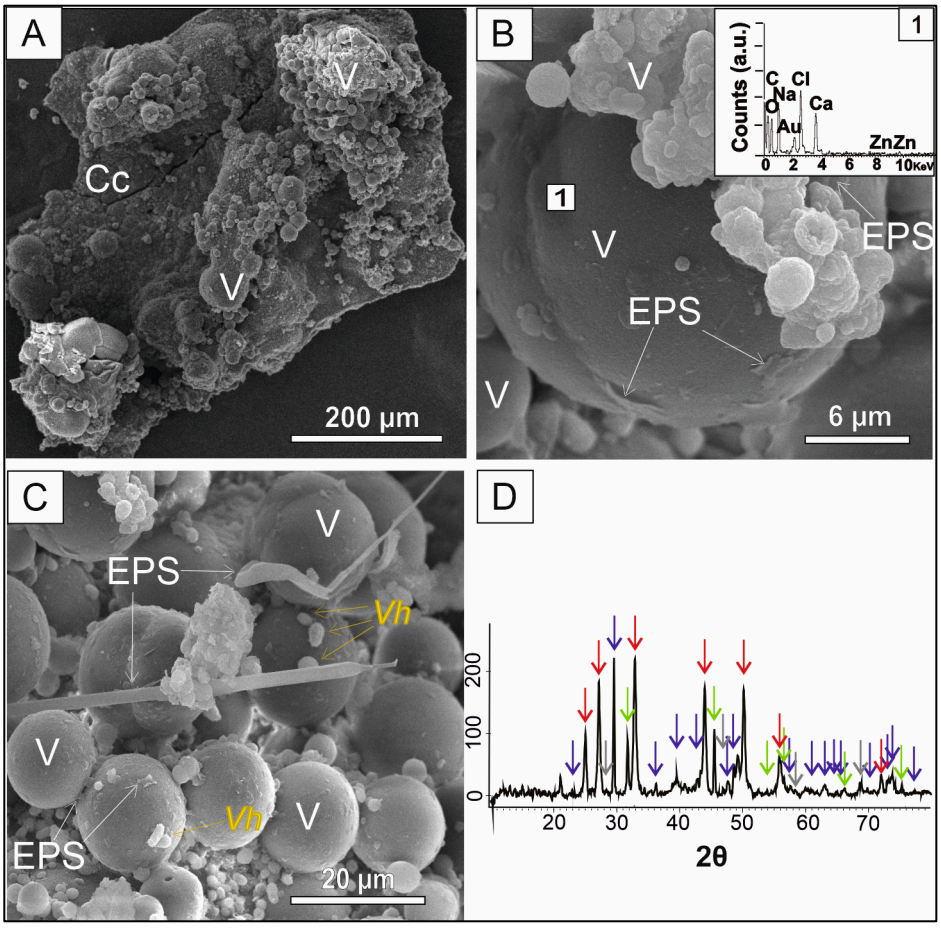

Figure 4. SEM micrographs showing aggregates of vaterite and calcite. (**A**) vaterite crystal aggregates, exhibiting typical globular morphology, lying over calcite crust. (**B**) The surface of vaterite is covered by bacterial EPS remains and smaller globular carbonates. The EDX spectrum of vaterite formed from Zn-spiked solutions is shown on the right upper corner of the Figure 1. (**C**) Bacterial cells (*Vibrio harveyi*) and EPS remains closely associated with vaterite crystals. (**D**) X-ray diffraction pattern of precipitates formed on vaterite and calcite precipitated from Zn-bearing solutions: vaterite (red arrows), calcite (blue arrows), and halite (green arrows).V = vaterite; Cc = calcite cristals; EPS = bacterial esopolysaccharides.

4. Conclusions

Results show the ability of *V. harveyi* to co-precipitate calcium carbonates together with Cd, Cr, Pb, and Zn contributing to the immobilization of these metals. Calcite was produced from solutions containing Cd, Cr, and Pb, whereas vaterite was the dominant mineral phase precipitated from the Zn-spiked solutions. Vaterite globular aggregates did not exhibit dissolution features on their surface, like calcite crystals, in which Cd, Cr, and Pb were included, despite calcite is known as the most stable $CaCO_3$ polymorph and vaterite as the most soluble one. All this implies an inversion of the energetic stability between $CaCO_3$ polymorphs produced in presence of different heavy metals.

These results are interesting both from a theoretical and practical standpoint. The high heavy metal resistance showed by *Vibrio harveyi*, together with its ability to carry out MICP in such harsh conditions, points out the maintenance of carbon anhydrase and urease enzyme production in presence of, at least, 100 ppm of Cd Cr b or Zn, making this bacterium particularly useful in metal decontamination of heavy polluted environmental matrices. Heavy metal toxicity not only results from modification in the conformational arrangement of cellular polymers, or by interference with cell respiration, but also by the perturbation of osmotic balance. *Vibrio harveyi* known halophilic feature allows this

bacterium to withstand high osmotic pressure, adding an additional peculiarity to its array of metabolic characteristics [51].

In addition, the different carbonate minerals, formed in presence of different heavy metals, underline the feasibility of bioremediation of natural systems polluted with heavy metals, by allowing them to be included in carbonate minerals. The process appears to be rather effective and fast, as a mean of 97.2% of the 4 heavy metals studied here were included in carbonate minerals after 2 days of incubation, thanks to the activity of *V. harveyi*. This biotechnology should be based on a microorganism easy to be isolated and cultivated and able to precipitate conspicuous amounts of carbonate minerals in a short run. Being the kinetic of co-precipitation of calcium carbonates and heavy metals rather fast, the process of bio-remediation should be as short as possible in order to avoid that mechanisms of microbial dissolution of carbonate crystals could interfere with mineral precipitation.

Author Contributions: Conceptualization, M.A.J.; methodology, M.A.J., P.D.B., E.C. and V.P.; software, P.D.B.; formal analysis, M.A.J.; investigation, P.D.B., E.C. and V.P.; resources, M.E.S.-M. and V.P.; writing—original draft, M.A.J., P.D.B. and S.D.; writing—review and editing, M.E.S.-M. and S.D.; supervision, M.E.S.-M. and S.D.; project administration, M.A.J. All authors have read and agreed to the published version of the manuscript.

Funding: This research received no external funding.

Data Availability Statement: Not Applied.

Acknowledgments: The authors are indebted to Gaetano Ricchezza for his technical support. MESM and PB acknowledge the support of the Research group UCM-910404.

Conflicts of Interest: The authors declare no conflict of interest.

References

1. Martin, M.H. *Biological Monitoring of Heavy Metal Pollution: Land and Air*; Springer Science & Business Media: London, UK, 2012.
2. Medfu Tarekegn, M.; Zewdu Salilih, F.; Ishetu, A.I. Microbes are used as a tool for the bioremediation of heavy metals from the environment. *Cogent Food Agric.* **2020**, *6*, 1783174. [CrossRef]
3. Prasad, M.N.V.; Hagemeyer, J.; Rengel, Z. Heavy metals as essential nutrients. In *Heavy Metal Stress in Plants: From Molecules to Ecosystems*; Springer: Nedlands, WA, USA, 1999; pp. 231–251.
4. Dumontet, S.; Dinel, H.; Schnitzer, M.; Paré, T.; Scopa, A. Composting organic residues: Trace metals and microbial pathogens. *Can. J. Soil Sci.* **2001**, *81*, 357–367. [CrossRef]
5. Poli, A.; Salerno, A.; Laezza, G.; di Donato, P.; Dumontet, S.; Nicolaus, B. Heavy metal resistance of some thermophiles: Potential use of α-amylase from Anoxybacillus amylolyticus as a microbial enzymatic bioassay. *Res. Microbiol.* **2009**, *160*, 99–106. [CrossRef] [PubMed]
6. Mishra, S.; Bharagava, R.N.; More, N.; Yadav, A.; Zainith, S.; Mani, S.; Chowdhary, P. Heavy Metal Contamination: An Alarming Threat to Environment and Human Health. In *Environmental Biotechnology: For Sustainable Future*; Springer: Singapore, 2018; pp. 103–125. [CrossRef]
7. Srivastava, S.; Goyal, P. *Novel Biomaterials: Decontamination of Toxic Metals from Wastewater*; Springer Science & Business Media: London, UK, 2010.
8. Tchounwou, P.B.; Yedjou, C.G.; Patlolla, A.K.; Sutton, D.J. Heavy metal toxicity and the environment. In *Molecular, Clinical and Environmental Toxicology: Volume 3: Environmental Toxicology*; Springer: Basel, Switzerland, 2012; pp. 133–164.
9. Li, Z.Y.; Ma, Z.W.; van der Kuijp, T.J.; Yuan, Z.W.; Huang, L. A review of soil heavy metal pollution from mines in China: Pollution and health risk assessment. *Sci. Total Environ.* **2014**, *468–469*, 843–853. [CrossRef]
10. Mohod, C.V.; Dhote, J. Review of heavy metals in drinking water and their effect on human health. *Int. J. Innov. Res. Sci. Eng. Technol.* **2013**, *2*, 2992–2996.
11. Aprile, A.; De Bellis, L. Editorial for the special issue "Heavy metals accumulation, toxicity, and detoxification in plants". *Int. J. Mol. Sci.* **2020**, *21*, 4103. [CrossRef]
12. Tovar-Sánchez, E.; Hernández-Plata, I.; Martinez, M.S.; Valencia-Cuevas, L.; Galante, P.M. Heavy metal pollution as a biodiversity threat. In *Heavy Metals*; Springer: Mexico, Mexico, 2018; p. 383.
13. Abdu, N.; Abdullahi, A.A.; Abdulkadir, A. Heavy metals and soil microbes. *Environ. Chem. Lett.* **2017**, *15*, 65–84. [CrossRef]
14. Nagajyoti, P.C.; Lee, K.D.; Sreekanth, T.V.M. Heavy metals, occurrence and toxicity for plants: A review. *Environ. Chem. Lett.* **2010**, *8*, 199–216. [CrossRef]
15. Pandey, G.; Madhuri, S. Heavy metals causing toxicity in animals and fishes. *Res. J. Anim. Vet. Fish. Sci.* **2014**, *2*, 17–23.
16. Verma, R.; Vijayalakshmy, K.; Chaudhiry, V. Detrimental impacts of heavy metals on animal reproduction: A review. *J. Entomol. Zool. Stud.* **2018**, *6*, 27–30.

17. Jaishankar, M.; Tseten, T.; Anbalagan, N.; Mathew, B.B.; Beeregowda, K.N. Toxicity, mechanism and health effects of some heavy metals. *Interdiscip. Toxicol.* **2014**, *7*, 60–72. [CrossRef] [PubMed]
18. Abbas, S.H.; Ismail, I.M.; Mostafa, T.M.; Sulaymon, A.H. Biosorption of heavy metals: A review. *J. Chem. Sci. Technol.* **2014**, *3*, 74–102.
19. Das, N.; Vimala, R.; Karthika, P. Biosorption of heavy metals–an overview. *Indian J. Biotechnol.* **2008**, *7*, 159–169.
20. Jarwar, M.A.; Dumontet, S.; Pasquale, V.; Chen, C. Microbial Induced Carbonate Precipitation: Environments, Applications, and Mechanisms. *Geomicrobiol. J.* **2022**, *39*, 833–851. [CrossRef]
21. Rehman, Z.U.; Junaid, M.F.; Ijaz, N.; Khalid, U.; Ijaz, Z. Remediation methods of heavy metal contaminated soils from environmental and geotechnical standpoints. *Sci. Total. Environ.* **2023**, *867*, 161468. [CrossRef]
22. He, Z.; Xu, Y.; Wang, W.; Yang, X.; Jin, Z.; Zhang, D.; Pan, X. Synergistic mechanism and application of microbially induced carbonate precipitation (MICP) and inorganic additives for passivation of heavy metals in copper-nickel tailings. *Chemosphere* **2023**, *311*, 136981. [CrossRef]
23. Kominko, H.; Gorazda, K.; Wzorek, Z. Effect of sewage sludge-based fertilizers on biomass growth and heavy metal accumulation in plants. *J. Environ. Manag.* **2022**, *305*, 114417. [CrossRef]
24. Logan, T.J.; Traina, S.J. Trace metals in agricultural soils. In *Metals in Groundwater*; CRC Press: Boca Raton, FL, USA, 2020; pp. 309–347.
25. Latosińska, J.; Kowalik, R.; Gawdzik, J. Risk Assessment of Soil Contamination with Heavy Metals from Municipal Sewage Sludge. *Appl. Sci.* **2021**, *11*, 548. [CrossRef]
26. Zeng, Y.; Chen, Z.; Lyu, Q.; Cheng, Y.; Huan, C.; Jiang, X.; Yan, Z.; Tan, Z. Microbiologically induced calcite precipitation for in situ stabilization of heavy metals contributes to land application of sewage sludge. *J. Hazard. Mater.* **2023**, *441*, 129866. [CrossRef] [PubMed]
27. Peng, D.; Qiao, S.; Luo, Y.; Ma, H.; Zhang, L.; Hou, S.; Wu, B.; Xu, H. Performance of microbial induced carbonate precipitation for immobilizing Cd in water and soil. *J. Hazard. Mater.* **2020**, *400*, 123116. [CrossRef] [PubMed]
28. Crawford, R.J.; Harding, I.H.; Mainwaring, D.E. Adsorption and coprecipitation of multiple heavy metal ions onto the hydrated oxides of iron and chromium. *Langmuir* **1993**, *9*, 3057–3062. [CrossRef]
29. Cruz, J.A.; Sánchez-Pastor, N.; Gigler, A.M.; Fernández-Díaz, L. Vaterite Stability in the Presence of Chromate. *Spectrosc. Lett.* **2011**, *44*, 495–499. [CrossRef]
30. Pérez-Garrido, C.; Fernández-Díaz, L.; Pina, C.M.; Prieto, M. In situ AFM observations of the interaction between calcite $(10\bar{1}4)$ surfaces and Cd-bearing aqueous solutions. *Surf. Sci.* **2007**, *601*, 5499–5509. [CrossRef]
31. Sánchez-Pastor, N.; Cruz, J.A.; Gigler, A.M.; Park, S.; Jordan, G.; Schmal, W.; Fernández-Díaz, L. Microprobe and Raman investigation of the zoning in synthetic (CO_3, CrO_4) crystals. *Macla* **2010**, *13*, 197–198.
32. Llera, A.R.; Jimenez, A.; Fernández-Díaz, L. Removal of Pb from Water: The Effectiveness of Gypsum and Calcite Mixtures. *Minerals* **2021**, *11*, 66. [CrossRef]
33. Bai, H.; Liu, D.; Zheng, W.; Ma, L.; Yang, S.; Cao, J.; Lu, X.; Wang, H.; Mehta, N. Microbially-induced calcium carbonate precipitation by a halophilic ureolytic bacterium and its potential for remediation of heavy metal-contaminated saline environments. *Int. Biodeterior. Biodegrad.* **2021**, *165*, 105311. [CrossRef]
34. Podda, F.; Zuddas, P.; Minacci, A.; Pepi, M.; Baldi, F. Heavy metal coprecipitation with hydrozincite $[Zn_5(CO_3)_2(OH)_6]$ from mine waters caused by photosynthetic microorganisms. *Appl. Environ. Microbiol.* **2000**, *66*, 5092–5098. [CrossRef]
35. Wang, M.; Wu, S.; Yang, Y.; Chen, F. Microbial induced carbonate precipitation and its application for immobilization of heavy metals: A review. *Res. Environ. Sci.* **2018**, *31*, 206–214.
36. Angeles, I.B.; Romero-Martínez, M.L.; Cavaliere, M.; Varrella, S.; Francescangeli, F.; Piredda, R.; Mazzocchi, M.G.; Montresor, M.; Schirone, A.; Delbono, I.; et al. Encapsulated in sediments: eDNA deciphers the ecosystem history of one of the most polluted European marine sites. *Environ. Int.* **2023**, *172*, 107738. [CrossRef] [PubMed]
37. Marchesi, J.R.; Sato, T.; Weightman, A.J.; Martin, T.A.; Fry, J.C.; Hiom, S.J.; Wade, W.G. Design and evaluation of useful bacterium-specific PCR primers that amplify genes coding for bacterial 16S rRNA. *Appl. Environ. Microbiol.* **1998**, *64*, 795–799. [CrossRef] [PubMed]
38. Chianese, E.; Tirimberio, G.; Riccio, A. PM2.5 and PM10 in the urban area of Naples: Chemical composition, chemical properties and influence of air masses origin. *J. Atmos. Chem.* **2019**, *76*, 151–169. [CrossRef]
39. Hu, X.; Fu, X.; Pan, P.; Lin, L.; Sun, Y. Incorporation of Mixing Microbial Induced Calcite Precipitation (MICP) with Pretreatment Procedure for Road Soil Subgrade Stabilization. *Materials* **2022**, *15*, 6529. [CrossRef]
40. Omoregie, A.I.; Palombo, E.A.; Nissom, P.M. Bioprecipitation of calcium carbonate mediated by ureolysis: A review. *Environ. Eng. Res.* **2020**, *26*, 200379. [CrossRef]
41. Pan, L.; Li, Q.; Zhou, Y.; Song, N.; Yu, L.; Wang, X.; Xiong, K.; Yap, L.; Huo, J. Effects of different calcium sources on the mineralization and sand curing of $CaCO_3$ by carbonic anhydrase-producing bacteria. *RSC Adv.* **2019**, *9*, 40827–40834. [CrossRef]
42. Seifan, M.; Samani, A.K.; Berenjian, A. Induced calcium carbonate precipitation using Bacillus species. *Appl. Microbiol. Biotechnol.* **2016**, *100*, 9895–9906. [CrossRef] [PubMed]
43. Torres-Aravena, Á.E.; Duarte-Nass, C.; Azócar, L.; Mella-Herrera, R.; Rivas, M.; Jeison, D. Can microbially induced calcite precipitation (MICP) through a ureolytic pathway be successfully applied for removing heavy metals from wastewater? *Crystals* **2018**, *8*, 438. [CrossRef]

44. Jacobson, A.D.; Wu, L. Microbial dissolution of calcite at T = 28 °C and ambient pCO2. *Geochim. et Cosmochim. Acta* **2009**, *73*, 2314–2331. [CrossRef]
45. Perito, B.; Mastromei, G. Molecular basis of bacterial calcium carbonate precipitation. In *Molecular Biomineralization: Aquatic Organisms Forming Extraordinary Materials*; Springer: Firenze, Italy, 2011; pp. 113–139.
46. Ehrlich, H.L. How microbes influence mineral growth and dissolution. *Chem. Geol.* **1996**, *132*, 5–9. [CrossRef]
47. Johnston, V.; Martín-Pérez, A.; Skok, S.; Mulec, J. Microbially-mediated carbonate dissolution and precipitation; towards a protocol for ex-situ, cave-analogue cultivation experiments. *Int. J. Speleol.* **2021**, *50*, 137–155. [CrossRef]
48. Welch, S.A.; Vandevivere, P. Effect of microbial and other naturally occurring polymers on mineral dissolution. *Geomicrobiol. J.* **1994**, *12*, 227–238. [CrossRef]
49. Fiore, S.; Dumontet, S.; Huertas, F.J.; Pasquale, V. Bacteria-induced crystallization of kaolinite. *Appl. Clay Sci.* **2011**, *53*, 566–571. [CrossRef]
50. Hiebert, F.K.; Bennett, P.C. Microbial control of silicate weathering in organic-rich groundwater. *Science* **1992**, *258*, 278–281. [CrossRef] [PubMed]
51. Wang, J.; Zhao, Y.; Li, D.; Qi, P.; Gao, X.; Guo, N.; Meng, R.; Tucker, M.E.; Yan, H.; Han, Z. Extreme halophilic bacteria promote the surface dolomitization of calcite crystals in solutions with various magnesium concentrations. *Chem. Geol.* **2022**, *606*, 120998. [CrossRef]
52. Han, Z.; Qi, P.; Zhao, Y.; Guo, N.; Yan, H.; Tucker, M.E.; Zhao, H. High Mg/Ca molar ratios promote protodolomite precipitation induced by the extreme halophilic bacterium Vibrio harveyi QPL$_2$. *Front. Microbiol.* **2022**, *13*, 821968. [CrossRef]
53. Sharma, M.; Satyam, N.; Reddy, K.R.; Chrysochoou, M. Multiple heavy metal immobilization and strength improvement of contaminated soil using bio-mediated calcite precipitation technique. *Environ. Sci. Pollut. Res.* **2022**, *29*, 51827–51846. [CrossRef] [PubMed]
54. Mwandira, W.; Nakashima, K.; Kawasaki, S. Bioremediation of lead-contaminated mine waste by Pararhodobacter sp. based on the microbially induced calcium carbonate precipitation technique and its effects on strength of coarse and fine grained sand. *Ecol. Eng.* **2017**, *109*, 57–64. [CrossRef]
55. Mugwar, A.J.; Harbottle, M.J. Toxicity effects on metal sequestration by microbially-induced carbonate precipitation. *J. Hazard. Mater.* **2016**, *314*, 237–248. [CrossRef]
56. Li, M.; Cheng, X.; Guo, H.; Yang, Z. Biomineralization of Carbonate by Terrabacter Tumescens for Heavy Metal Removal and Biogrouting Applications. *J. Environ. Eng.* **2016**, *142*, C4015005. [CrossRef]
57. Kim, Y.; Kwon, S.; Roh, Y. Effect of divalent cations (Cu, Zn, Pb, Cd, and Sr) on microbially induced calcium carbonate precipitation and mineralogical properties. *Front. Microbiol.* **2021**, *12*, 646748. [CrossRef] [PubMed]
58. Jalilvand, N.; Akhgar, A.; Alikhani, H.A.; Rahmani, H.A.; Rejali, F. Removal of Heavy Metals Zinc, Lead, and Cadmium by Biomineralization of Urease-Producing Bacteria Isolated from Iranian Mine Calcareous Soils. *J. Soil Sci. Plant Nutr.* **2019**, *20*, 206–219. [CrossRef]
59. Kang, B.; Zha, F.; Li, H.; Xu, L.; Sun, X.; Lu, Z. Bio-Mediated Method for Immobilizing Copper Tailings Sand Contaminated with Multiple Heavy Metals. *Crystals* **2022**, *12*, 522. [CrossRef]
60. He, J.; Chen, X.; Zhang, Q.; Achal, V. More effective immobilization of divalent lead than hexavalent chromium through carbonate mineralization by Staphylococcus epidermidis HJ2. *Int. Biodeterior. Biodegrad.* **2019**, *140*, 67–71. [CrossRef]
61. Liu, R.; Lian, B. Non-competitive and competitive adsorption of Cd^{2+}, Ni^{2+}, and Cu^{2+} by biogenic vaterite. *Sci. Total. Environ.* **2018**, *659*, 122–130. [CrossRef]
62. Sánchez-Pastor, N.; Gigler, A.M.; Cruz, J.A.; Park, S.H.; Jordan, G.; Fernández-Díaz, L. Growth of calcium carboante in the presence of Cr (VI). *Cryst. Growth Des.* **2011**, *11*, 3081–3089. [CrossRef]
63. Navrotsky, A. Energetic clues to pathways to biomineralization: Precursors, clusters, and nanoparticles. *Proc. Natl. Acad. Sci. USA* **2004**, *101*, 12096–12101. [CrossRef] [PubMed]
64. Radha, A.V.; Forbes, T.Z.; Killian, C.E.; Gilbert, P.U.P.A.; Navrotsky, A. Transformation and crystallization energetics of synthetic and biogenic amorphous calcium carbonate. *Proc. Natl. Acad. Sci. USA* **2010**, *107*, 16438–16443. [CrossRef] [PubMed]